Chemical Engineering and Processing 79 (2014) 7–13

Contents lists available at ScienceDirect

Chemical Engineering and Processing: Process Intensification

journal homepage: www.elsevier.com/locate/cep

Numerical investigation of CH_4/O_2 mixing in Y-shaped mesoscale combustors with/without porous media

Yi Liu, Jingyi Zhang, Aiwu Fan*, Jianlong Wan, Hong Yao, Wei Liu

State Key Laboratory of Coal Combustion, Huazhong University of Science and Technology, Wuhan 430074, China

ARTICLE INFO

Article history:
Received 22 November 2013
Received in revised form 20 January 2014
Accepted 6 March 2014
Available online 15 March 2014

Keywords:
Mesoscale combustor
Y-shaped channel
Porous media
Mixing enhancement
Mass dispersion effect

ABSTRACT

A good mixing of reactants is important for non-premixed combustion in miniature combustors. In this paper, mixings of methane and oxygen in Y-shaped mesoscale combustors with and without porous media were compared numerically. The results show that when there is no porous media in the horizontal channel, the mixing becomes worse with the decrease of the included angle between two inlets, or with the increase of inlet velocity. The reason is that for the case without porous media, the dominant mixing mechanism is molecular diffusion under concentration gradients. In contrast, for the case with porous media, due to the mass dispersion effect which becomes more significant with the decrease of channel width, satisfactory mixing can always be attained in the Y-shaped mesoscale combustor. Moreover, fairly good mixing can still be achieved in the horizontal channel of shorter length. All these demonstrate that the porous media greatly promotes the methane/oxygen mixing in the Y-shaped mesoscale combustor, which is beneficial for flame stabilization. Meanwhile, the combustor dimension can be further scaled down because good mixing is possible in the channel with even smaller included angle and shorter length. This is very important for the application of miniature power generation system.

© 2014 Elsevier B.V. All rights reserved.

1. Introduction

With the rapid development of micro-electromechanical systems (MEMS), the demands for appropriate portable power generators are growing. The high energy densities of hydrocarbon fuels make it possible for combustion-based micro power generation systems to drive the MEMS in the future [1–3]. Therefore, micro combustion has drawn extensive attention in the past decades.

However, there are some critical challenges to sustain a stable combustion in miniature combustors. Those adversities include the increased heat losses due to large surface area-to-volume ratio of the combustor chamber and the reduced residence time of the fuel/oxidant mixture. To achieve a complete reaction in micro- and meso-scale combustors, premixed combustion is superior to non-premixed combustion. Thus, premixed combustion under small scale has been widely investigated experimentally and numerically [4–22]. However, although premixed combustion is beneficial for a complete conversion in miniature combustors, it still has some shortcomings. First, premixed combustion needs a separate fuel/oxidizer mixer which makes the whole system more complicated. In addition, premixed flame is prone to flashback which gives rise to a potential safety problem for users of portable micro power generators. In contrast, non-premixed combustion does not have such demerits. Therefore, non-premixed combustion also gained extensive attentions from researchers.

As the Reynolds number in micro- and meso-scale combustors is relatively low, the molecular diffusion is the dominant mechanism for fuel/oxidizer mixing, which is always unable to achieve a good mixing for a continuous flame and a complete reaction. For instance, Miesse et al. [23–25] experimentally investigated the diffusion flames in a Y-shaped micro-burner and they observed multiple isolated flame cells. Since the fuel conversion degree when the flame cells are present is poor, it represents an undesirable mode of combustion in terms of efficient micro-burner operation. To reveal the mechanisms responsible for these discrete flamelets, Xu and Ju [26] studied the non-premixed flames in a heated rectangular channel with a gap distance of 6 mm and a width of 100 mm. Fuel and air were fed into the channel via two horizontally parallel inlet ports. By controlling the flow velocity and wall temperature, a 'flame street' that consists of multiple flamelets inside the mixing layer was observed, which is similar to that reported by Miesse et al. [23–25]. They pointed out that onset of the 'flame street' was due to the process of diffusion and re-ignition. Therefore, for high combustion efficiency, it is critical to promote the mixing

* Corresponding author at: State Key Laboratory of Coal Combustion, Huazhong University of Science and Technology, 1037 Luoyu Road, Wuhan 430074, China. Tel.: +86 27 87542618; fax: +86 27 87540724.
E-mail addresses: faw_73@163.com, faw@hust.edu.cn (A. Fan).

http://dx.doi.org/10.1016/j.cep.2014.03.002
0255-2701/© 2014 Elsevier B.V. All rights reserved.

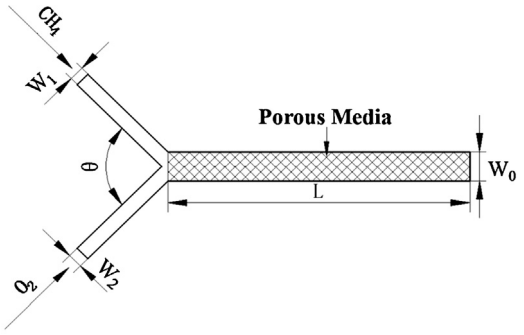

Fig. 1. Schematic of the Y-shaped mesoscale combustor.

process of fuel and oxidizer in micro- and meso-scale combustors.

It is well known that porous media combustion has been proved to be a good approach to stabilize flame under unfavorable conditions, such as very lean mixture [27]. Porous media has also been implied to stabilize premixed flame in micro- and meso-scale combustors [28–30]. However, the application of porous media to non-premixed combustion was seldom reported. Due to the mass dispersion effect of the porous media, it is expected that fuel/oxidizer mixing can be greatly enhanced for non-premixed combustion. Being limited by the size, it is very difficult to obtain information inside a micro-combustor by systematic experimental studies. On the other hand, numerical simulation provides a convenient and cost-effective approach to investigate mixing and combustion phenomena in small channels and the underlying mechanisms. Thus, in the present work, we numerically investigate methane/oxygen mixing in a Y-shaped mesoscale channel with and without porous media. The impacts of the included angle between methane and oxygen inlets, inlet velocity and channel length are addressed.

2. Numerical technique

2.1. Geometric model

The two dimensional Y-shaped combustor is schematically illustrated in Fig. 1. It consists of two inlet channels, i.e., fuel and oxygen flow paths, and a horizontal channel for mixing and combustion. The widths of the two inlet channels (W_1, W_2) are both 2 mm and the included angle between them (θ) is varied from 30° to 150°. The horizontal channel is of 40 mm in length (L) and 4 mm in width (W_0). The porosity of the porous media is 0.52.

2.2. Governing equations

The gas phase is treated as an incompressible fluid with constant physical properties. The conservation equations of continuity, momentum and gaseous species are expressed as follows.

Continuity equation:

$$\frac{\partial(\phi\rho_g)}{\partial t} + \nabla(\phi\rho_g u) = 0 \tag{1}$$

where ϕ, ρ_g, and u are the porosity of porous media, the density of the gas and the gas velocity, respectively. Gas densities are computed from the ideal gas equation of state for a multi-component mixture.

Momentum equation:

$$\frac{\partial(\phi\rho_g u)}{\partial t} + \nabla(\phi\rho_g uu) = -\phi\cdot p + \nabla(\phi\tau) + S \tag{2}$$

where p is the hydrostatic pressure, τ is the viscous stress tensor and S is the source term in the momentum equation. For a homogeneous porous media, S can be described as

$$S = -\left(u\cdot\frac{\mu}{\alpha} + \frac{1}{2}C_2\rho_g|u|u\right) \tag{3}$$

Here, α represents the permeability and C_2 stands for the inertial resistance factor; μ is the dynamic viscosity; α and C_2 which are derived from the Ergun equation are described as follows [31].

$$\alpha = \frac{D_p^2}{150}\frac{\phi^3}{(1-\phi)^2} \tag{4}$$

$$C_2 = \frac{3.5}{D_p}\frac{(1-\phi)}{\phi^3} \tag{5}$$

where D_p is the mean pore diameter.

The source term is composed of two parts which are viscous loss term (the first term on the right-hand side) and inertial loss term (the second term on the right-hand side).

Species conservation equation:

$$\phi\rho_g\cdot\frac{\partial Y_i}{\partial t} + \nabla(\phi\rho_g uY_i) = \nabla(\phi\rho_g\cdot D\cdot\nabla Y_i) + \phi\omega_i W_i \tag{6}$$

where Y_i is the mass fraction, V_i is the diffusion velocity, W_i is the molecular weight, and ω_i is the production rate of the i^{th} species, respectively. The production term can be eliminated due to the cold state under investigation. Then the equation can be simplified to the following form:

$$\phi\rho_g\cdot\frac{\partial Y_i}{\partial t} + \nabla(\phi\rho_g uY_i) = \nabla(\phi\rho_g\cdot D\cdot\nabla Y_i) \tag{7}$$

The diffusion coefficient involving mass dispersion effect is given below [32].

$$D = D_{im} + D_m^d \tag{8}$$

Here, the first term D_{im} is the diffusion coefficient of the i^{th} component into the mixture, while the second term D_m^d is the mass dispersion coefficient. The precise mass dispersion correlation on species dilution is still unknown. In the present work, we adopt the analogous formula below [32].

$$\frac{D_m^d}{D_{im}} = 0.5Pe_m \tag{9}$$

$$D_{im} = \frac{1-X_i}{\sum_N^{j\neq i}(X_j/D_{ij})} \tag{10}$$

where D_{ij} is the binary diffusion coefficient, and X_i or X_j is the mole fraction of the i^{th} or j^{th} component. Pe_m is the mass transfer Peclet number [33].

$$Pe_m = \frac{\tau_{diff}}{\tau_{conv}} \tag{11}$$

According to Broadwell et al. [34], τ_{diff} and τ_{conv} are defined as follows:

$$\tau_{diff} = \frac{l_{diff}}{D} \tag{12}$$

$$\tau_{conv} = \frac{M}{U} \tag{13}$$

where l_{diff} is the characteristic scale of molecular diffusion, M is the characteristic scale of the channel (for the present work, it is the channel width, W_0), D is the molecular diffusion coefficient, and U is the average velocity.

As the characteristic scale of the mesoscale combustor under investigation is still much larger than the molecular free path, the Knudsen number is far less than 0.001 and thus no-slip boundary condition for velocity is applied. The maximum average velocity in

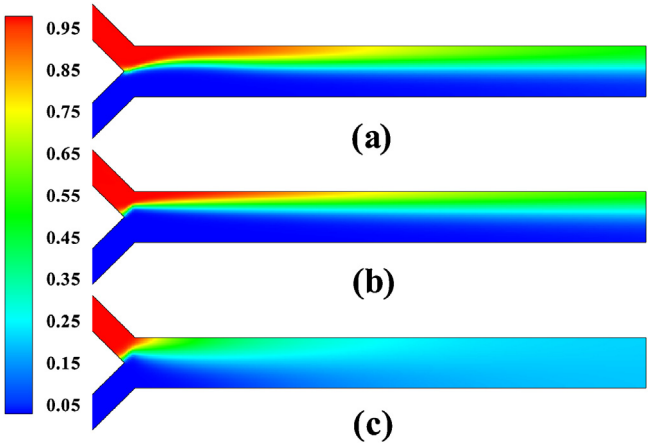

Fig. 2. Mass fraction contours of methane in the Y-shaped mesoscale combustor at $\theta = 90^{\circ}$, $\phi = 1.0$, $V_{CH_4} = 1.0$ m/s: (a) without porous media, (b) with porous media and ignoring the mass dispersion effect, (c) with porous media and considering the mass dispersion effect.

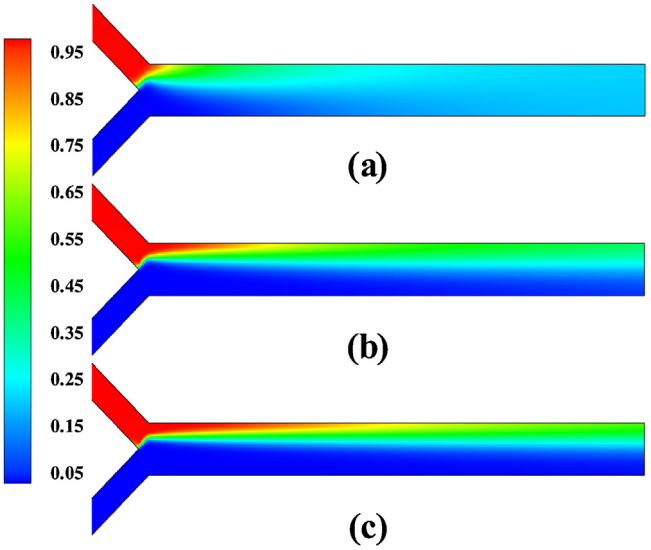

Fig. 3. Mass fraction contours of methane in the Y-shaped channels filled with porous medial at different channel widths: (a) $W_0 = 4$ mm, (b) $W_0 = 20$ mm, (c) $W_0 = 40$ mm. The length to width ratio of the horizontal channel is fixed for the three geometrical models. For the convenience of comparison, the two macroscale channels are scaled down to the same size as the mesoscale channel. Other parameters are set to be: $\theta = 90^{\circ}$, $\phi = 1.0$ and $V_{CH_4} = 1.0$ m/s.

the combustor chamber is confined to be less than 5.8 m/s, therefore, the flow without porous media is laminar. While the porous media is applied, the Reynolds number determined by the diameter of pores (3×10^{-4} m) is less than 100. According to Pedras [35], the flow is in the Forchheimer regime ($1–10 < Re < 150$). Therefore, laminar model is adopted in the present work for the simulation with porous media.

2.3. Computation method

Methane and oxygen were selected as the fuel and oxidant, respectively. Uniform velocity distributions were specified at the two inlets of the mesoscale combustor. An outflow boundary condition was specified at the exit. The computational fluid dynamics (CFD) software package FLUENT 6.3 [36] was applied to solve the mass, momentum and species conservation equations. The second-order upwind scheme was used to discretize the model, and the "SIMPLE" algorithm was employed to couple the pressure and velocity. A non-uniform square grid system with 20,221 meshes was employed in the computation and the results were verified to be grid-independent. A user-defined function was introduced to take the mass dispersion effect into consideration in the porous media zone. The convergence of the CFD simulation was judged based on the residuals of all governing equations. The results obtained in this study were achieved with residuals smaller than 1.0×10^{-6}.

3. Results and discussion

In the following, we first compare the mixing processes in the smooth channel with the porous media case. The mass dispersion effect of the porous media is examined and the impact of combustor scale on mass dispersion is especially investigated. Then, the effects of several factors such as the included angle between two inlets, inlet velocity, and channel length are studied.

3.1. Effect of mass dispersion on the mixing process in the mesoscale channel with porous media

The mass fraction contours of methane in the Y-shaped mesoscale combustors with/without porous media are shown in Fig. 2. The included angle between the two inlets is 90° in this case. The inlet velocities for methane and oxygen flows are 1 m/s and 2 m/s, respectively (corresponds to an equivalence ratio $\phi = 1.0$). It is seen from Fig. 2a that there is a clear interface with large gradient between the methane and oxygen sides, which implies that the mixing is unsatisfactory. The interface remains horizontal and extends to the combustor exit. This indicates that in the Y-shaped combustor without porous media, except for the collision at leading edge of mixing interface, the dominant mixing mechanism is molecular diffusion which is not able to achieve a perfect mixing within a short distance. Fig. 2b depicts the mass fraction contours of methane in the combustor with porous media but ignoring the mass dispersion effect. It is noted from Fig. 2b that the interface with large gradient of mass fraction is also observed, as that shown in Fig. 2a. However, when the dispersion effect is considered, the mixing layer with large concentration gradients vanishes, which indicates that the mixing of methane and oxygen is much more rapid due to the mass dispersion effect, as clearly seen from Fig. 2c. The mass fraction of methane grows fairly uniform at the midstream of the horizontal channel. This is because the complicated structure of porous media makes the fluid passageways mazy and the fluid velocity varies in both magnitudes and directions everywhere. These facts demonstrate that the molecular diffusion is the dominant mechanism for the mixing process in smooth channel, while the mass dispersion effect is significant for the mixing process in the mesoscale channel filled with porous media. This can be easily deduced from the comparison between the mass dispersion coefficient D_m^d and molecular diffusion coefficient D_{im} in Eq. (9). The order of D_m^d is 10^{-4} while the order of D_{im} is about 10^{-5}.

We now examine the mass dispersion effect on the mixing process in the channels with different widths. The channel widths of two other cases were selected to be $W_0 = 20$ mm and 40 mm. The length to width ratio of the horizontal channel was kept to be the same as the original case. The inlet velocity of methane is 1.0 m/s and the equivalence ratio is 1.0. The porosity and pore size of the porous media are the same for the three cases. Fig. 3 shows mass fraction contours of methane in these three channels, in which the mass dispersion effect was included in the numerical simulation. It is seen from Fig. 3 that as the channel width changes from mesoscale to macroscale, the interface with large CH_4 concentration gradient becomes longer. In other words, the methane/oxygen mixing gets worse with the increase of channel width. This means

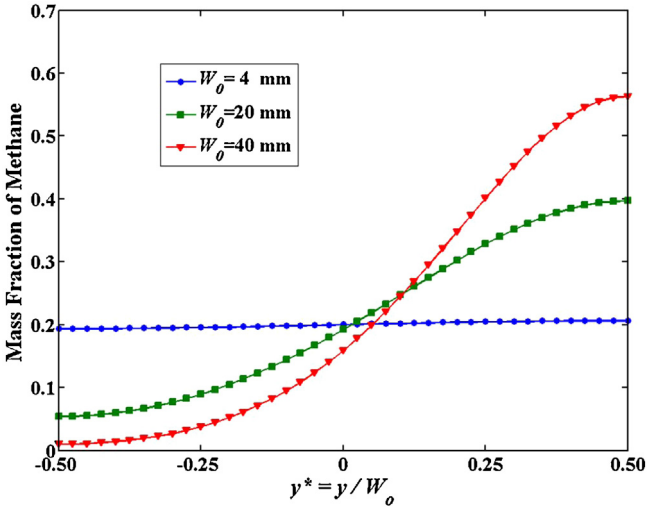

Fig. 4. Mass fraction profiles of methane at the combustor exit for different channel widths. There is porous media in the horizontal channel and $\theta = 90^\circ$, $\phi = 1.0$, V_{CH_4} = 1.0 m/s.

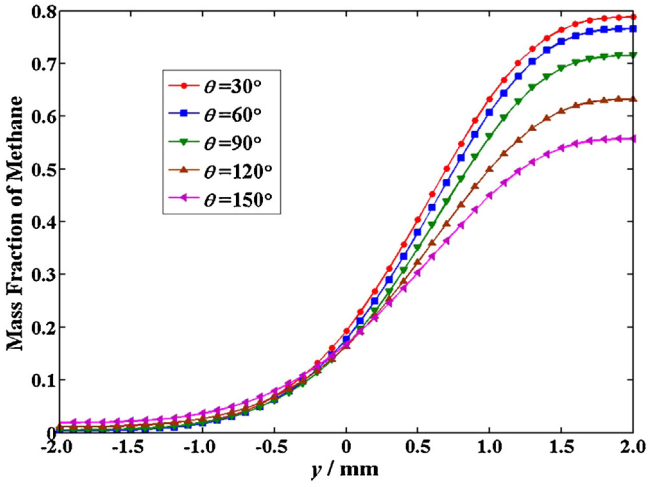

Fig. 5. Mass fraction profiles of methane at the combustor exit for different included angles. There is no porous media in the horizontal channel and $\phi = 1.0$, V_{CH_4} = 2.0 m/s.

that the mass dispersion effect grows weaker in macroscale channel. The reason is explained as follows. According to Eqs. (13) and (11), τ_{conv} is proportional to the channel width W_0, which results in the decrease of Pe_m when the channel width is increased. Consequently, the mass dispersion coefficient D_m^d is reduced with the decrease of Pe_m based on Eq. (9). Therefore, when the channel width is increased from 4 mm to 20 mm and 40 mm, the mass dispersion coefficient is reduced to 1/5 and 1/10 of that of the 4-mm wide channel. This implies that the mass dispersion effect is greatly weakened in macroscale channel with porous media.

To quantitatively evaluate the eventual mixing effect of methane and oxygen, we plot the mass fraction profile of methane at the combustor exit in Fig. 4. In this figure, y^* is the dimensionless coordinate at the combustor exit, with a positive direction pointing upward from the center. It is seen from Fig. 4 that for the channel with a width of 4 mm, the methane mass fraction is nearly a horizontal line around 0.2. This implies a perfect mixing (the methane mass fraction of the ideal pre-mixture is 0.20) is attained in this case. For the 20 mm wide channel, the mass fraction of methane is only 0.05 at the downside of the exit, climbing up to 0.4 at the topside, which indicates an uneven distribution of methane at the combustor exit. As the channel width is increased to 40 mm, the mass fraction of methane at the combustor exit becomes more uneven. Therefore, it is more beneficial to adopt porous media in mesoscale combustors than macroscale combustors.

3.2. Effect of the included angle

Fig. 5 presents the mass fraction profiles of methane at the combustor exit for various included angles. In these cases, there is no porous media in the horizontal channel and the inlet velocity of methane V_{CH_4} is 2.0 m/s. This figure demonstrates that as the included angle increases, the methane concentration grows more uniform at the combustor exit, implying a better mixing at larger included angles. The reason is explained below.

It is easy to know from Fig. 1 that the inlet velocity u can be decomposed into a horizontal component, u_x, and a vertical component, u_y, which are expressed as follows:

$$u_x = u \times \cos\frac{\theta}{2} \tag{14}$$

$$u_y = u \times \sin\frac{\theta}{2} \tag{15}$$

As we know that the mixing of fuel and oxygen mainly depends on two factors, one is the collision intensity at the leading edge of the horizontal channel, while the other is the residence time of reactants. From Eqs. (14) and (15) it can be deduced that, as the included angle is less than 180° and thus $\theta/2 < 90^\circ$, when the included angle is increased, the vertical velocity component is correspondingly increased whereas the horizontal velocity component is decreased. Therefore, the collision between the two streams is intensified and the residence time is extended simultaneously, which implies that a better mixing can be accomplished at a large included angle. However, one should be aware that the vertical dimension of the Y-shaped combustor becomes bigger as well. Thus, an excessive large included angle is not recommended because a smaller size is always desirable for MEMS.

The effect of the included angel on the mixing in the combustor with porous media is illustrated in Fig. 6. It is evident from Fig. 6 that perfect mixing of methane and oxygen can be achieved at any angle due to the dispersion effect caused by the porous media. The corresponding velocity contours are depicted in Fig. 7, which demonstrates that all the velocity fields in the porous media are uniform and similar for all the cases with different included angles. This is because the porous media can rectify the non-uniform incoming flows to a uniform one. In summary, the included angle

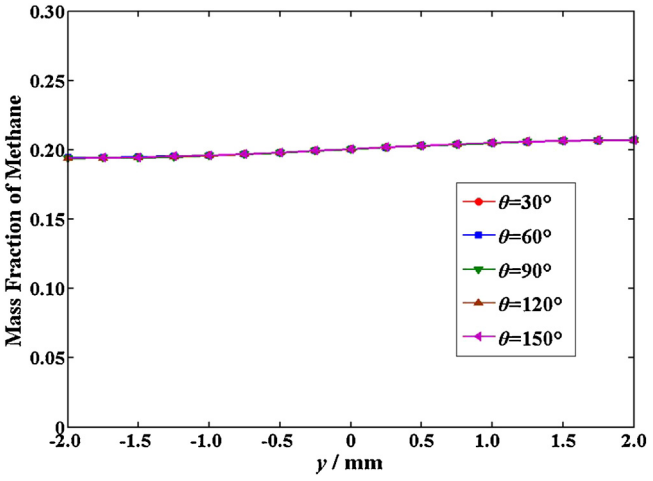

Fig. 6. Mass fraction profiles of methane at the combustor exit for different included angles. There is porous media in the horizontal channel and $\phi = 1.0$, V_{CH_4} = 2.0 m/s.

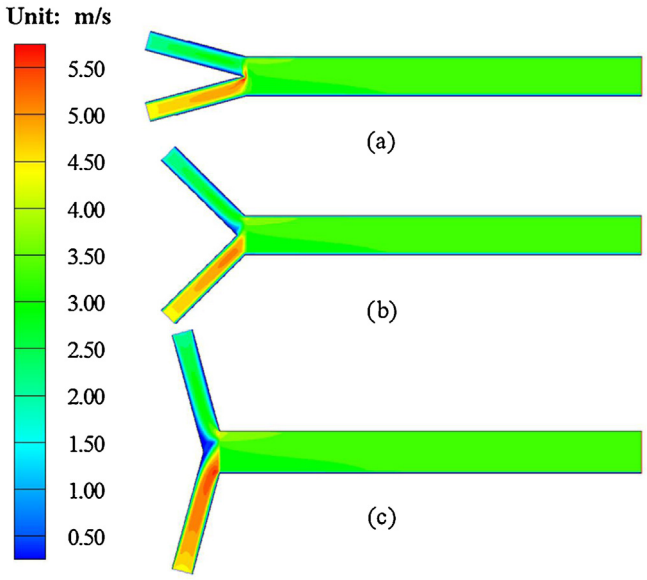

Fig. 7. Contours of velocity magnitude in the Y-shaped mesoscale combustor for different included angles: (a) $\theta = 30^\circ$, (b) $\theta = 90^\circ$, (c) $\theta = 150^\circ$. There is porous media in the horizontal channel and $\phi = 1.0$, $V_{CH_4} = 2.0$ m/s.

has a negligible effect on the methane/oxygen mixing when porous media is applied, which also means that the scale of the whole combustor can be reduced.

3.3. Effect of the inlet velocity

In this section, we investigate the effect of the inlet velocity on the methane/oxygen mixing in the channels with/without porous media. The inlet velocity of methane takes the values of 0.2 m/s, 0.4 m/s, 0.6 m/s, 0.8 m/s and 1.0 m/s. The corresponding velocities of oxygen are 0.4 m/s, 0.8 m/s, 1.2 m/s, 1.6 m/s and 2.0 m/s, respectively. The included angle between the two inlets is set to be 90° and the equivalence ratio maintains unity.

Fig. 8 shows the mass fraction profiles of methane at the combustor exit for different inlet velocities in the absence of porous media. It is seen from Fig. 8 that when the inlet velocity is decreased, the mass fraction profile of methane becomes more uniform. To illustrate the differences of mixing processes for different inlet velocities, we present the mass fraction contours of methane for $V_{CH_4} = 0.2$ m/s, 0.6 m/s and 1.0 m/s in Fig. 9. From this figure it is

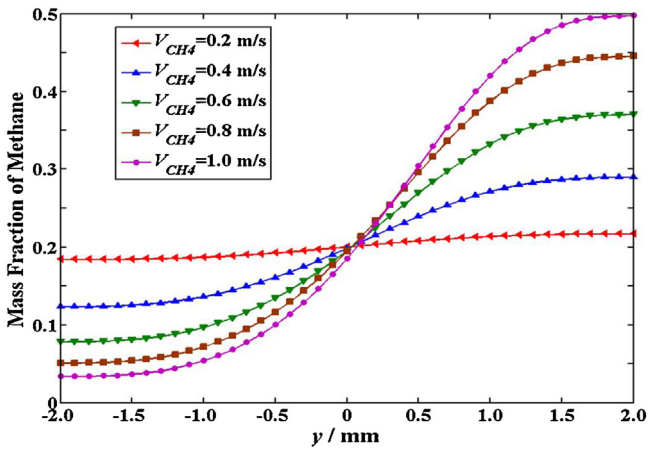

Fig. 8. Mass fraction profiles of methane at the combustor exit for different inlet velocities. There is no porous media in the horizontal channel and $\theta = 90^\circ$, $\phi = 1.0$.

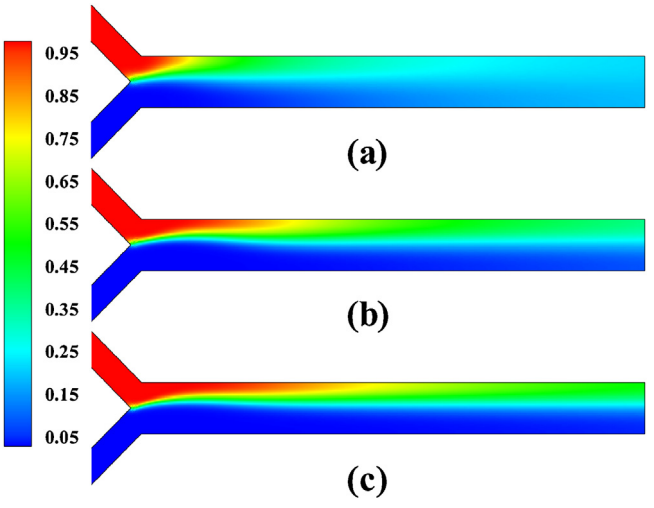

Fig. 9. Mass fraction contours of methane in the Y-shaped mesoscale combustor for different inlet velocities: (a) $V_{CH_4} = 0.2$ m/s, (b) $V_{CH_4} = 0.6$ m/s, (c) $V_{CH_4} = 1.0$ m/s. There is no porous media in the horizontal channel and $\theta = 90^\circ$, $\phi = 1.0$.

clearly seen that on the upper side, the methane concentration decreases more rapidly as the inlet velocity is decreased. When the inlet velocity of methane is 0.2 m/s, mass fraction contours of methane is nearly uniform at the combustor exit, which is consistent with Fig. 8. However, for relatively higher inlet velocity, the methane–oxygen interface extends until the combustor exit, which indicates unsatisfactory mixing in these cases. These demonstrate that when there is no porous medium in the horizontal channel, the dominant mixing mechanism is molecular diffusion, while the effect of convection on the mixing process is indirect. It can be deduced from Eq. (14) that the horizontal velocity component u_x is proportional to the inlet velocity u. Therefore, the residence time is inversely proportional to the inlet velocity u. In other words, when the inlet velocity is lower, methane and oxygen have a longer residence time to mix with each other and a better mixing is possible. Nevertheless, for the cases without porous media in the horizontal channel, good mixing can only be achieved at very low inlet velocities, e.g., 0.2 m/s.

Fig. 10 presents the mass fraction profiles of methane at the combustor exit for different inlet velocities when the horizontal channel is filled with porous media. This figure shows that there

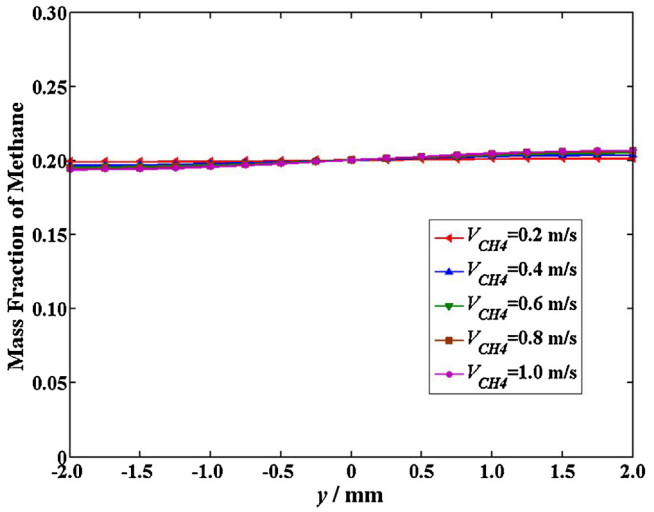

Fig. 10. Mass fraction profiles of methane at the combustor exit for different inlet velocities. There is porous media in the horizontal channel and $\theta = 90^\circ$, $\phi = 1.0$.

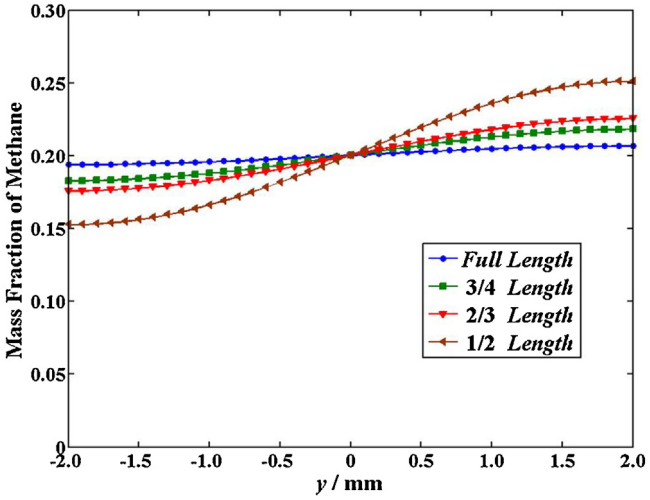

Fig. 11. Mass fraction profiles of methane at the combustor exit for different lengths of the horizontal channel. There is porous media in the horizontal channel and $\theta = 90^{\circ}$, $\phi = 1.0$, $V_{CH_4} = 1.0$ m/s.

are only small differences between these profiles. For example, the differences between the methane mass fractions of these cases on the same side are less than 0.006; meanwhile, the largest difference between methane mass fractions of the upper and lower side is only around 0.013. These indicate that in the cases with porous media in the horizontal channel, the mass dispersion effect is always the dominant mechanism for methane/oxygen mixing, which can ensure a good mixing even at high inlet velocities.

3.4. Effect of the channel length

Fig. 11 illustrates the mass fraction profiles of methane at the combustor exit for different lengths of the horizontal channel with porous media. It is seen from this figure that when the length of horizontal channel is reduced to half of the original length, the difference between the mass fractions of methane at the upper and lower ends of the combustor exit reaches 0.1, which indicates that the mixing of this case is not that good as the full length case. However, when the length of horizontal channel is reduced to 3/4 and 2/3 of the full length, fairly good mixing can still be attained for these two cases. These can be clearly seen from Fig. 12 in which the mass fraction contours of methane for different channel lengths are illustrated. Thus, dimension of the original Y-shaped mesoscale combustor can be reduced by great extent, which is of special importance for mini-power generators which always have size limitations.

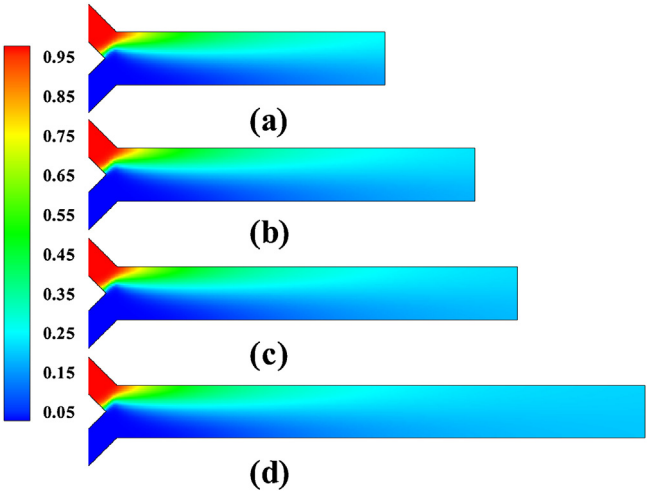

Fig. 12. Mass fraction contours of methane in the Y-shaped mesoscale combustors for different lengths of the horizontal channel: (a) 1/2 of full length, (b) 2/3 of full length, (c) 3/4 of full length, (d) full length. There is porous media in the horizontal channel and $\theta = 90^{\circ}$, $\phi = 1.0$, $V_{CH_4} = 1.0$ m/s.

4. Conclusions

In the present work, mixings of methane and oxygen in Y-shaped mesoscale combustors with and without porous media were numerically investigated and compared. Results reveal that for the case without porous media in the horizontal channel, the mixing effect becomes worse with the decrease of the included angle between two inlet channels, or with the increase of inlet velocity. A good mixing cannot be achieved except for the cases with very low inlet velocity. This is because when there is no porous media in the horizontal channel, the dominant mixing mechanism is molecular diffusion under concentration gradients, which is always not able to achieve a good mixing. On the contrary, for the cases with porous media in the horizontal channel, the mass dispersion effect is more significant than molecular diffusion under micro- and meso-scales, which ensures that a satisfactory mixing can always be attained. Furthermore, fairly good mixing can still be accomplished in the horizontal channel of reduced length. All these demonstrate that the porous media significantly enhances the methane/oxygen mixing in the Y-shaped mesoscale combustor, which is beneficial for flame stabilization. In addition, the combustor dimension can be further scaled down because good mixing is possible in the horizontal channel with even smaller included angle and/or shorter length. This is of special importance for the application of miniature power generation system.

Acknowledgement

This work was supported by the National Natural Science Foundation of China under Grant Number of 51276073.

References

[1] A.C. Fernandez-Pello, Micropower generation using combustion: issues and approaches, Proc. Combust. Inst. 29 (2002) 883–899.
[2] Y.G. Ju, K. Maruta, Microscale combustion: technology development and fundamental research, Prog. Energy Combust. Sci. 37 (2011) 669–715.
[3] K. Maruta, Micro and mesoscale combustion, Proc. Combust. Inst. 33 (2011) 125–150.
[4] K. Maruta, T. Kataoka, N.I. Kim, S. Minaev, R. Fursenko, Characteristics of combustion in a narrow channel with a temperature gradient, Proc. Combust. Inst. 30 (2005) 2429–2436.
[5] S. Minaev, E. Sereshchenko, R. Fursenko, A.W. Fan, K. Maruta, Splitting flames in a narrow channel with temperature gradient in the walls, Combust. Expl. Shock Waves 45 (2009) 119–125.
[6] A.W. Fan, S. Minaev, E. Sereshchenko, Y. Tsuboi, H. Oshibe, H. Nakamura, K. Maruta, Propagation dynamics of splitting flames in a heated microchannel, Combust. Expl. Shock Waves 45 (2009) 245–250.
[7] S. Kumar, K. Maruta, S. Minaev, Pattern formation of flames in radial microchannels with lean methane–air mixtures, Phys. Rev. E 75 (2007) 016208.
[8] S. Kumar, K. Maruta, S. Minaev, On the formation of multiple rotating pleton-like flame structures in radial microchannels with lean methane–air mixtures, Proc. Combust. Inst. 31 (2007) 3261–3268.
[9] A.W. Fan, S. Minaev, S. Kumar, W. Liu, K. Maruta, Regime diagrams and characteristics of flame patterns in radial microchannels, Combust. Flame 153 (2008) 479–489.
[10] A.W. Fan, S. Minaev, E. Sereshchenko, R. Fursenko, S. Kumar, W. Liu, K. Maruta, Experimental and numerical investigations of flame pattern formations in a radial microchannel, Proc. Combust. Inst. 32 (2009) 3059–3066.
[11] N.I. Kim, S. Aizumi, T. Yokomori, S. Kato, T. Fujimori, K. Maruta, Development and scale effects of small Swiss-roll combustors, Proc. Combust. Inst. 31 (2007) 3243–3250.
[12] C.H. Kuo, P.D. Ronney, Numerical modeling of non-adiabatic heat-recirculating combustors, Proc. Combust. Inst. 31 (2007) 3277–3284.

[13] G.A. Boyarko, C.J. Sung, S.J. Schneider, Catalyzed combustion of hydrogen-oxygen in platinum tubes for micro-propulsion applications, Proc. Combust. Inst. 30 (2005) 2481–2488.
[14] W.M. Yang, S.K. Chou, C. Shu, Z.W. Li, H. Xue, Combustion in micro-cylindrical combustors with and without a backward facing step, Appl. Therm. Eng. 22 (2002) 1777–1787.
[15] B. Khandelwal, G.P.S. Sahota, S. Kumar, Investigation into the flame stability limits in a backward step micro scale combustor with premixed methane–air mixtures, J. Micromech. Microeng. 20 (2010) 095030.
[16] G.P.S. Sahota, B. Khandelwal, S. Kumar, Experimental investigation on a new active swirl based microcombustor for an integrated micro-reformer system, Energy Convers. Manage. 52 (2011) 3206–3213.
[17] M. Akram, S. Kumar, Experimental studies on dynamics of methane–air premixed flame in meso-scale diverging channels, Combust. Flame 158 (2011) 915–924.
[18] J.L. Wan, A.W. Fan, K. Maruta, H. Yao, W. Liu, Experimental and numerical investigation on combustion characteristics of premixed hydrogen/air flame in a micro-combustor with a bluff body, Int. J. Hydrogen Energy 37 (2012) 19190–19197.
[19] A.W. Fan, J.L. Wan, K. Maruta, H. Yao, W. Liu, Interactions between heat transfer, flow field and flame stabilization in a micro-combustor with a bluff body, Int. J. Heat Mass Transfer 66 (2013) 72–79.
[20] A.W. Fan, J.L. Wan, Y. Liu, B.M. Pi, H. Yao, K. Maruta, W. Liu, The effect of the blockage ratio on the blow-off limit of a hydrogen/air flame in a planar micro-combustor with a bluff body, Int. J. Hydrogen Energy 38 (2013) 11438–11445.
[21] U.W. Taywade, A.A. Deshpande, S. Kumar, Thermal performance of a micro combustor with heat recirculation, Fuel Process. Technol. 109 (2013) 179–188.
[22] A.W. Fan, J.L. Wan, Y. Liu, H. Yao, W. Liu, Effect of bluff body shape on the blow-off limit of hydrogen/air flame in a planar micro-combustor, Appl. Therm. Eng. 62 (2014) 13–19.
[23] C.M. Miesse, R.I. Masel, C.D. Jensen, M.A. Shannon, M. Short, Submillimeter-scale combustion, AIChE J. 50 (2004) 3206–3214.
[24] C.M. Miesse, R.I. Masel, M. Short, M.A. Shannon, Diffusion flame instabilities in a 0.75 mm non-premixed microburner, Proc. Combust. Inst. 30 (2005) 2499–2507.
[25] C.M. Miesse, R.I. Masel, M. Short, M.A. Shannon, Experimental observations of methane–oxygen diffusion flame structure in a sub-millimetre microburner, Combust. Theory Model. 9 (2005) 77–92.
[26] B. Xu, Y.G. Ju, Experimental studies of flame street in a mesoscale channel, in: 5th US Combustion Meeting, San Diego, USA, 2007.
[27] M.A. Mujeebu, M.Z. Abdullah, M.Z.A. Bakar, A.A. Mohamad, M.K. Abdullah, Applications of porous media combustion technology—a review, Appl. Energy 86 (2009) 1365–1375.
[28] T. Marbach, A. Agrawal, A mesoscale combustor using annular porous inert media for heat recirculation, in: 43rd AIAA Aerospace Sciences Meeting and Exhibit, Reno, Nevada, January 10–13, 2005.
[29] J. Li, S.K. Chou, Z.W. Li, W.M. Yang, Experimental investigation of porous media combustion in a planar micro-combustor, Fuel 89 (2010) 708–715.
[30] K. Xu, M.H. Liu, P.H. Zhao, Stability of lean combustion in mini-scale porous media combustor with heat recuperation, Chem. Eng. Process.: Process Intensif. 50 (2011) 608–613.
[31] S. Ergun, Fluid flow through packed columns, Chem. Eng. Prog. 48 (1952) 89–94.
[32] M.R. Henneke, J.L. Ellzey, Modeling of filtration combustion in a packed bed, Combust. Flame 117 (1999) 832–840.
[33] K.H.J. Dellimore, Investigation of Fuel–Air Mixing in a Micro-Flameholder for Micro-power and Scramjet Applications (Master thesis), University of Maryland, 2005.
[34] J. Broadwell, R. Briedenthal, A simple model of mixing and chemical reaction in a turbulent shear layer, J. Fluid Mech. 125 (1982) 397–410.
[35] M.H.J. Pedras, M.J.S. de Lemos, Macroscopic turbulence modeling for incompressible flow through undeformable porous media, Int. J. Heat Mass Transfer 44 (2001) 1081–1093.
[36] Fluent 6.3 User's Guide, Fluent Inc., Lebanon, NH, 2006.